# Theory of electron liquids. II. Static and dynamic form factors, correlation energy, and plasmon dispersion

Naoki Iwamoto* and Eckhard Krotscheck†
*Institute for Theoretical Physics, University of California, Santa Barbara, California 93106*

David Pines
*Department of Physics, University of Illinois at Urbana—Champaign, Urbana, Illinois 61801*
(Received 19 September 1983)

We use the Ceperley and Alder Green's-function Monte Carlo data for the static form factor, $S(q)$, of an electron liquid to calculate the static local-field correction, $G(q)$, to the dielectric function which takes into account short-range electron correlations. The resulting local-field correction in the long-wavelength limit is obtained by smoothly fitting to the results of Iwamoto and Pines, which are exact in this limit. We use the $G(q)$ thus obtained to calculate the static and dynamic form factors, the contribution to the correlation energy from different momentum transfers, plasmon dispersion, and the plasmon-dispersion coefficient. We compare these theoretical quantities with the available experimental data, and use the $\omega^3$-sum rule (which we also calculate from the Monte Carlo data) to discuss the limitations arising from the use of the static local-field correction.

## I. INTRODUCTION

This is the second of a planned series of papers[1–3] in which we study the dielectric properties of an electron liquid by combining the best currently available microscopic data on the ground-state properties from the Green's-function Monte Carlo calculations[4] with exact sum rules and physical arguments to obtain the self-consistent fields responsible for the local-field corrections and particle-hole effective mass. In the first paper[1] (hereafter referred to as IP) electron-hole configuration and momentum-space pseudopotentials were introduced to describe the way in which short-range charge- and spin-induced correlations between electrons act to modify, at short distances, the Coulomb interaction between electrons of parallel and antiparallel spin. Use was made of the interpolation formula given by Vosko, Wilk, and Nusair[5] for the spin-dependent correlation energy, which these authors obtained from the Green's-function Monte Carlo data of Ceperley and Alder,[4] to calculate the compressibility and the static spin susceptibility. The IP pseudopotentials were constructed in such a way that they led to local-field corrections to the static response functions, which ensured that these quantities reduced to the Monte Carlo results in the long-wavelength limit. These pseudopotentials provide physical insight into the similarities among electron liquids, helium liquids in the polarization potential model,[6] and a dilute hard-sphere Fermi gas.

In the present paper we explore two further ways to obtain local-field corrections for a wide range of momentum transfers directly from the Monte Carlo data for the ground state of an electron liquid. Our theory is phenomenological in the sense that the Monte Carlo calculations may be viewed as very clean "computer experiments," in which the electron liquid is not disturbed by solid-state effects. Thus we are able to sort out the effects of intrinsic electron-electron correlations before including more complicated effects. The *microscopic* foundation of our theory may be found in the Fermi hypernetted chain (FHNC) theory[7] of quantum liquids and the theory of correlated basis functions[8] (CBF) as its extension to excited states. A recent study of the connection between the random-phase approximation (RPA) and the "chain diagrams" in FHNC theory[9] provides the formal basis of the present study.

Purely microscopic theories for the ground state of quantum fluids, especially for an electron liquid, are presently in a quite satisfactory state. It is certainly premature to make the same statement about excited states. The broad contact[9] between purely microscopic theories, based on correlated wave functions[8] and the more phenomenological polarization-potential theory,[6] allows one to alternate conveniently between both pictures. However, purely microscopic approaches do have the disadvantage that one must accept whatever results the ground-state calculations yield. Even in the relatively well-understood electron gas case, this is not always satisfactory.[10] Pseudopotentials, such as the ones introduced by Aldrich and Pines[6] for $^3$He, or by IP for electron liquids, have the distinctive advantage that the "effective interactions" used there may be adjusted to the empirical data, while the structure of the microscopic theory is maintained.

In the present paper we carry through a *minimum* program in this direction. We show how local pseudopotentials may be constructed which reproduce the static form factors in the density and spin channels, obtained "empirically" by Monte Carlo simulations. Multipair excitations are, in this study, not taken explicitly into account. We use the $\omega^3$-sum rule to demonstrate the shortcomings of theories which do not take these into account.

In carrying out our program, we use the "mean spheri-

 

cal approximation,"[11] which allows us to express pseudopotentials in a closed form in terms of the static form factors. This mean spherical approximation (MSA) is discussed and tested in Sec. II.

Using the MSA, we calculate, in Sec. III, the spin-symmetric and spin-antisymmetric local-field corrections, and compare these with the results of the IP polarization-potential theory. We also calculate the corresponding quantity from the $\omega^3$-sum rule, and discuss the role played by multipair excitations in the latter. In Sec. IV we calculate the static form factor with various local-field corrections and determine as well the contributions to the correlation energy from different momentum transfers. In Sec. V we study the plasmon-dispersion relation and the dynamic form factor and compare these quantities with experimental data. A discussion and overview are given in Sec. VI.

## II. RESPONSE FUNCTIONS AND THE MEAN SPHERICAL APPROXIMATION

In examining the dielectric properties of an electron liquid it is useful to introduce two response functions:[12] the linear density-density response function $\chi(q,\omega)$, which describes the response of the system to an external longitudinal field, and the screened response function $\chi_{sc}(q,\omega)$, which describes the response to the sum of an external longitudinal field and the induced polarization field. By definition, these response functions are related through

$$\chi(q,\omega)=\frac{\chi_{sc}(q,\omega)}{1-(4\pi e^2/q^2)\chi_{sc}(q,\omega)} . \tag{2.1}$$

Then, the dielectric function may be written as

$$\epsilon(q,\omega)=1-\frac{4\pi e^2}{q^2}\chi_{sc}(q,\omega) , \tag{2.2a}$$

$$\frac{1}{\epsilon(q,\omega)}=1+\frac{4\pi e^2}{q^2}\chi(q,\omega) . \tag{2.2b}$$

In the Hartree-Fock approximation, the electrons respond to the external field as free particles. Thus $\chi(q,\omega)$ is approximated by the free-electron (Lindhard) response function $\chi^0(q,\omega)$ (where HF represents Hartree-Fock):

$$\chi^{HF}(q,\omega)=\chi^0(q,\omega) , \tag{2.3a}$$

$$\frac{1}{\epsilon_{HF}(q,\omega)}=1+\frac{4\pi e^2}{q^2}\chi^0(q,\omega) . \tag{2.3b}$$

In the random-phase approximation, the electrons respond to the screened field (i.e., the sum of the external field and the polarization field) as free particles; thus $\chi_{sc}(q,\omega)$ is approximated by $\chi^0(q,\omega)$:

$$\chi_{sc}^{RPA}(q,\omega)=\chi^0(q,\omega) , \tag{2.4a}$$

$$\epsilon_{RPA}(q,\omega)=1-\frac{4\pi e^2}{q^2}\chi^0(q,\omega) . \tag{2.4b}$$

In order to take electron correlations into account, one may modify Eq. (2.4a) to

$$\chi_{sc}(q,\omega)=\frac{\chi^0(q,\omega)}{1-f_q^s\chi^0(q,\omega)}=\frac{\chi^0(q,\omega)}{1+v(q)G(q)\chi^0(q,\omega)} , \tag{2.5a}$$

and from Eq. (2.1),

$$\chi(q,\omega)=\frac{\chi^0(q,\omega)}{1-(4\pi e^2/q^2+f_q^s)\chi^0(q,\omega)}=\frac{\chi^0(q,\omega)}{1-v(q)[1-G(q)]\chi^0(q,\omega)} . \tag{2.5b}$$

Here, $f_q^s$ describes a potential designed to take into account the modification in the restoring force brought about by electron correlations which act to prevent electrons from sampling the full effect of the Coulomb interaction at short distances. It is therefore attractive. When combined with the bare potential $v(q)=4\pi e^2/q^2$, it leads to an effective potential:

$$v_{eff}^s(q)=\frac{4\pi e^2}{q^2}+f_q^s\equiv v(q)[1-G(q)] , \tag{2.6}$$

where the dimensionless function of $q$,

$$G(q)=-f_q^s/v(q) , \tag{2.7}$$

is called the *static local-field correction.*

From the linear-response function, one obtains the dynamic form factor $S(q,\omega)$ via the fluctuation-dissipation theorem:[13]

$$S(q,\omega)=-\frac{2\hbar}{n}\mathrm{Im}\chi(q,\omega), \quad \omega>0 \tag{2.8a}$$

$$=-\frac{\hbar q^2}{2\pi ne^2}\mathrm{Im}\frac{1}{\epsilon(q,\omega)}, \quad \omega>0 \tag{2.8b}$$

where $n$ is the electron number density. The *static form factor* is the frequency integral of $S(q,\omega)$,

$$S(q)\equiv\int_{-\infty}^{\infty}\frac{d\omega}{2\pi}S(q,\omega) \tag{2.9a}$$

$$=-\frac{2\hbar}{n}\int_0^{\infty}\frac{d\omega}{2\pi}\mathrm{Im}\left[\frac{\chi^0(q,\omega)}{1-v_{eff}^s(q)\chi^0(q,\omega)}\right] . \tag{2.9b}$$

Thus Eq. (2.9b) allows one to calculate $S(q)$ from a given $v_{eff}^s(q)$.

In similar fashion, one may introduce the spin-density response function, $\chi^I(q,\omega)$; the analog of (2.5b) is then

$$\chi^I(q,\omega)=\frac{\chi^0(q,\omega)}{1-f_q^a\chi^0(q,\omega)} , \tag{2.10}$$

so that the spin-antisymmetric effective potential is

$$v_{eff}^a(q)=f_q^a=-v(q)G^a(q) , \tag{2.11}$$

where $G^a(q)$ is the spin-antisymmetric static local-field correction. Similarly, the spin-antisymmetric, or spin-density, dynamic form factor is given by

$$S^a(q,\omega)=-\frac{2\hbar}{n}\mathrm{Im}\chi^I(q,\omega), \quad \omega>0 \tag{2.12}$$

while its frequency integral yields the static spin-antisymmetric structure factor,

$$S^a(q)=\int_{-\infty}^{\infty}\frac{d\omega}{2\pi}S^a(q,\omega) . \tag{2.13}$$

In IP, configuration-space pseudopotentials, $f^{\uparrow\uparrow}(r)$ and $f^{\uparrow\downarrow}(r)$, were introduced to describe the way in which electron correlations modify the Coulomb interaction at short distances. The quantities $f_q^s$ and $f_q^a$ were taken to be the spin-symmetric and spin-antisymmetric combinations of the corresponding momentum-space pseudopotentials,

$$f_q^s=\tfrac{1}{2}(f_q^{\uparrow\uparrow}+f_q^{\uparrow\downarrow}) , \tag{2.14a}$$

$$f_q^a=\tfrac{1}{2}(f_q^{\uparrow\uparrow}-f_q^{\uparrow\downarrow}) , \tag{2.14b}$$

and a simple Yukawa form was adopted for $f(r)$, so that

$$f_q^{\uparrow\uparrow}=-\frac{4\pi e^2}{q^2+q_{\uparrow\uparrow}^2} , \tag{2.15a}$$

$$f_q^{\uparrow\downarrow}=-\frac{4\pi e^2}{q^2+q_{\uparrow\downarrow}^2} . \tag{2.15b}$$

The screening wave vectors $q_{\uparrow\uparrow}$ and $q_{\uparrow\downarrow}$ were then chosen so that in the long-wavelength limit the static density-density linear response function $\chi(q,0)$ and static spin susceptibility $\chi^I(q,0)$ reduced to the exact limiting values calculated by Vosko, Wilk, and Nusair from the Monte Carlo calculations of Ceperley and Alder. The local-field corrections obtained by IP are thus

$$G_{\rm IP}(q)=\frac{1}{2}\left[\frac{q^2}{q^2+q_{\uparrow\uparrow}^2}+\frac{q^2}{q^2+q_{\uparrow\downarrow}}\right] , \tag{2.16a}$$

$$G_{\rm IP}^a(q)=\frac{1}{2}\left[\frac{q^2}{q^2+q_{\uparrow\uparrow}^2}-\frac{q^2}{q^2+q_{\uparrow\downarrow}^2}\right] , \tag{2.16b}$$

and their long-wavelength limits,

$$\lim_{q\to 0} G_{\rm IP}(q)=\frac{1}{2}\left[\frac{q^2}{q_{\uparrow\uparrow}^2}+\frac{q^2}{q_{\uparrow\downarrow}}\right] , \tag{2.17a}$$

$$\lim_{q\to 0} G_{\rm IP}^a(q)=\frac{1}{2}\left[\frac{q^2}{q_{\uparrow\uparrow}^2}-\frac{q^2}{q_{\uparrow\downarrow}^2}\right] , \tag{2.17b}$$

are exact, in that with the choices, Eq. (2.17), one is guaranteed, via Eqs. (2.5a) and (2.10), to obtain the Monte Carlo values of the compressibility and spin susceptibility.

The choice, Eqs. (2.16), for the local-field correction is but one of many possible choices. In the following section we consider two alternative choices. One choice, which we denote by $G_0(q)$ and $G_0^a(q)$, is made such that when one makes it and subsequently carries out the frequency integral, Eqs. (2.9a) and (2.13), one obtains the Monte Carlo values of $S(q)$ and $S^a(q)$. In this approach the determination of $G_0(q)$ and $G_0^a(q)$ may be considerably simplified with the aid of the *mean spherical approximation* (MSA), which is sometimes known as the "fluid dynamic" or "collective" approximation.[11,14,15]

The essence of the MSA is, as we will show in Appendix A, to approximate the propagator for the particle-hole excitations in the Lindhard function $\chi^0(q,\omega)$, by one with a single pole. A very thorough discussion of the MSA may be found in the recent work of Bishop and Lührmann.[11] It should be intuitively clear that such an approximation is justified whenever the low-lying excitations within the system are dominated by a collective mode. As shown in Appendix A, with the aid of the MSA one can carry out the integration in Eq. (2.9b) in closed form, and thereby obtain[16]

$$S(q)=\frac{S_F(q)}{\{1+(4mn/\hbar^2q^2)v_{\rm eff}^s(q)[S_F(q)]^2\}^{1/2}} , \tag{2.18}$$

where $S_F(q)$ is the static form factor in the Hartree-Fock approximation

$$S_F(q)=\begin{cases}\dfrac{3}{4}\left[\dfrac{q}{q_F}\right]-\dfrac{1}{16}\left[\dfrac{q}{q_F}\right]^3, & q\le 2q_F\\ 1, & q>2q_F\end{cases} \tag{2.19}$$

where $q_F$ is the Fermi wave number. The MSA is the underlying approximation[9] in variational theories of quantum fluids. It not only renders the above-mentioned frequency integral trivial, but in fact simplifies purely microscopic treatments of quantum liquids such that vast classes of diagrams can be easily summed. It is worth pointing out here that Eq. (2.18) gives in fact an excellent approximation to the static form factor if the effective interaction $v_{\rm eff}^s(q)$ is repulsive, while it gives a poor approximation for an attractive effective interaction.[17] This is, for example, the case in the spin channel[6] in liquid $^3$He.

The accuracy of the MSA may be tested by comparing, for a given $v_{\rm eff}^s(q)$, the static form factor obtained via the MSA, Eq. (2.18), with one obtained by the frequency integral (2.9b), where $\chi_0(q,\omega)$ is given by the Lindhard function, Eq. (2.4a). We shall see that the MSA is, for the (effective) interactions used in the electron gas, typically accurte within an error of $\sim 1\%$.

Generalizing the MSA (2.18) to spin-antisymmetric interactions one obtains

$$S^a(q)=\frac{S_F(q)}{\{1+(4mn/\hbar^2q^2)v_{\rm eff}^a(q)[S_F(q)]^2\}^{1/2}} , \tag{2.20}$$

where $v_{\rm eff}^a$ is given by Eq. (2.11).

Finally, we note that the MSA expression for $S(q)$ [Eq. (2.18)] is exact in both the long- and short-wavelength limits: For small $q$, Eq. (2.18) reduces to

$$\lim_{q\to 0} S(q)=\frac{\hbar q^2}{2m\omega_p} , \tag{2.21}$$

where $\omega_p=(4\pi ne^2/m)^{1/2}$ is the plasma frequency. This is the correct form of the plasmon contribution to $S(q)$; single pair and multipair contributions are proportional to $q^5$ and $q^4$, respectively, in this limit.[12]

For large $q$, Eq. (2.18) becomes

$$\lim_{q\to\infty} S(q)=1-\frac{8\pi mne^2}{\hbar^2q^4}[1-G_0(q)]+\cdots . \tag{2.22}$$

This is consistent with the large-$q$ behavior of $S(q)$ derived from the fluctuation-dissipation theorem [Eq. (2.9b)] by using the dielectric function of the form (2.2a) with (2.5a).[18] On the other hand, from the definition of the pair correlation function $g(r)$,

$$g(r)-1=\frac{1}{nV}\sum_{\vec q}[S(q)-1]e^{i\vec q\cdot\vec r} , \tag{2.23}$$

one obtains

$$\lim_{q\to\infty} S(q)=1-\frac{8\pi n}{q^4}g'(0)\ , \tag{2.24}$$

where $g'(0)$ is the derivative of the pair correlation function at zero interparticle distance. From the analysis of the $s$-wave Schrödinger equation in the $r\to 0+$ limit it is known that[18]

$$g'(0)=g(0)/a_B\ , \tag{2.25}$$

where $a_B$ is the Bohr radius. Thus from Eqs. (2.22), (2.24), and (2.25), one obtains

$$\lim_{q\to\infty} G_0(q)=1-g(0)\ . \tag{2.26}$$

This is the correct behavior of $G(q)$ for large $q$.[18–20]

## III. LOCAL-FIELD CORRECTIONS AND THE $\omega^3$-SUM RULE

### A. Local-field corrections

Conventional approaches to the electron liquid problem take the route of developing a theory for the local-field corrections[21,22] and using the functions $G(q)$,$G^a(q)$ to calculate the dynamic and static form factors. Now that the static form factor of the electron liquid is known quite accurately from the variational[23] and Green's-function Monte Carlo[4,24] calculations, one may take the opposite route and calculate $G(q)$ and $G^a(q)$ from the Monte Carlo data. In the present paper we shall take the latter approach. The calculation could, in principle, be performed by solving Eq. (2.9b) for $v^s_{\rm eff}(q)$, and a corresponding equation for $v^a_{\rm eff}(q)$. However, the MSA allows one to simplify this procedure: It yields directly an algebraic expression for the local-field corrections in terms of the known static form factors:

$$G_0(q)=1-\frac{3\pi}{16\alpha r_s}\left[\frac{q}{q_F}\right]^4\left[\frac{1}{[S(q)]^2}-\frac{1}{[S_F(q)]^2}\right]\ , \tag{3.1}$$

$$G^a_0(q)=-\frac{3\pi}{16\alpha r_s}\left[\frac{q}{q_F}\right]^4\left[\frac{1}{[S^a(q)]^2}-\frac{1}{[S_F(q)]^2}\right]\ . \tag{3.2}$$

Here, $\alpha=(4/9\pi)^{1/3}$, and $r_s=1/\alpha a_B q_F$. One difficulty in this procedure is that the functional relations (3.1) and (3.2), are very sensitive to small errors in $S(q)$ and $S^a(q)$, respectively, while the Monte Carlo data[24] are not completely accurate in the regime $q<\frac{1}{2}q_F$. We remedy this situation by employing at small $q$ the local-field corrections obtained in IP. There, it was shown that the local-field corrections are determined in the long-wavelength limit by exact boundary conditions derived from the compressibility and the static spin susceptibility. Therefore, the accuracy of the IP local-field corrections in this limit is guaranteed. In other words, the small-momentum behavior of $S(q)$ is known (see Ref. 1). Therefore, we use the IP local-field corrections in the region where the error bars of the Monte Carlo data are too large. This is typically in the regime $0<q<\frac{1}{2}q_F$. We note, however, that the IP local-field corrections are, of course, consistent with the Monte Carlo error bars. Results for $G_0(q)$ are shown in Figs. 1 and 2. In Fig. 1, one finds a peak structure in $G_0(q)$ at $q>2q_F$ for $r_s=1$ and 2, which disappears for $r_s=5$. We also show the quantity $(4\pi ne^2/q^2)G^a_0(q)$ for $r_s=1$, 2, and 5 in Fig. 3.

In calculating $G_0(q)$ [or $G^a_0(q)$] we have placed emphasis on the low-frequency end of the spectrum of $S(q,\omega)$, since $G_0(q)$ is determined from $S(q)$ via the MSA; as we shall see, when one substitutes $G_0(q)$ in the expression Eq. (2.9b) and carries out the integral therein, one recovers $S(q)$ to a high degree of accuracy. This approach

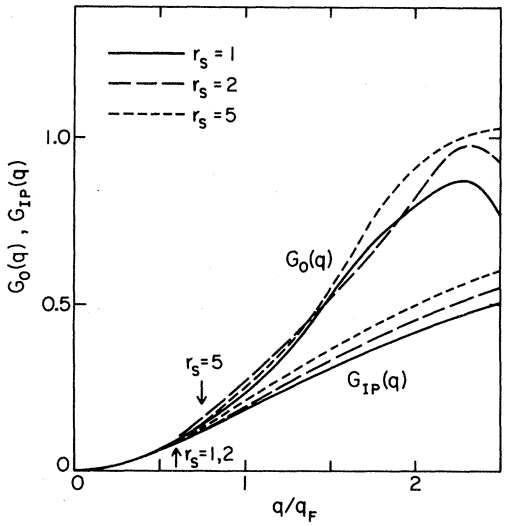


FIG. 1. Local-field correction $G_0(q)$ for $r_s=1$, 2, and 5. For large $q$, Eq. (3.1) with the Monte Carlo values for $S(q)$ was used, while for small $q$ the polarization-potential model (Ref. 1) was used. The arrows indicate the points of smooth fit. The lower curves show the local-field correction in the polarization-potential model, $G_{\rm IP}(q)$ (Ref. 1), for $r_s=1$, 2, and 5.

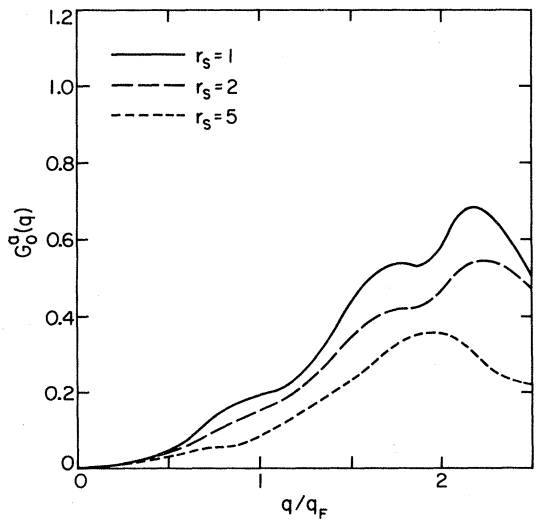


FIG. 2. Spin-antisymmetric local-field correction $G^a_0(q)$ for $r_s=1$, 2, and 5. The procedure is the same as in Fig. 1 except that Eq. (3.2) with the Monte Carlo values for $S^a(q)$ was used for large $q$.

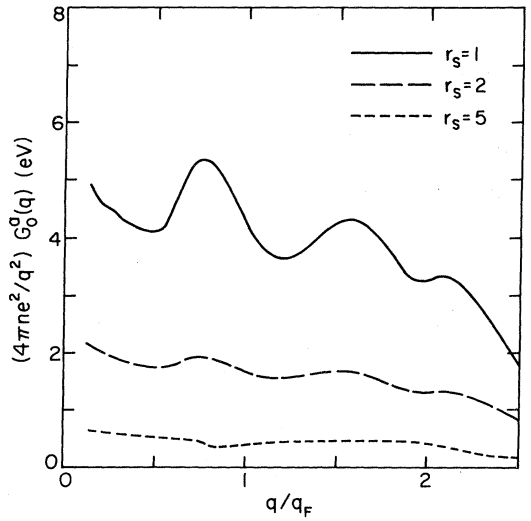


FIG. 3. Plot of $(4\pi ne^2/q^2)G_0^a(q)$ in units of eV for $r_s=1$, 2, and 5.

is, however, not the only way one might utilize the Monte Carlo data to obtain $G(q)$; an alternate approach is to determine $G(q)$ from the $\omega^3$-sum rule of Puff and Mihara,[25] and we consider that now.

### B. The $\omega^3$-sum rule

The linear-response function $\chi(q,\omega)$ may be expanded in the high-frequency limit as[25]

$$\lim_{\omega\to\infty}\chi(q,\omega)=\frac{\langle\omega^1\rangle}{\omega^2}+\frac{\langle\omega^3\rangle}{\omega^4}+\cdots . \tag{3.3}$$

The frequency moments

$$\langle\omega^{2l-1}\rangle\equiv-\int_{-\infty}^{\infty}\frac{d\omega}{\pi}\omega^{2l-1}\mathrm{Im}\chi(q,\omega) , \tag{3.4}$$

may be calculated exactly by using the commutator algebra of the Hamiltonian and the density operator. The first moment yields the $f$-sum rule,

$$\langle\omega^1\rangle=\frac{nq^2}{m} , \tag{3.5a}$$

while the third moment may be written in the form[22,25]

$$\langle\omega^3\rangle=\frac{nq^2}{m}\left[t_q^2+4\langle E_{\rm kin}\rangle\frac{t_q}{\hbar}+\omega_p^2[1-I(q)]\right] , \tag{3.5b}$$

where $t_q=\hbar q^2/2m$, $\langle E_{\rm kin}\rangle$ is the expectation value of the kinetic energy per particle for an interacting system, and

$$I(q)=-\frac{1}{N}\sum_{\vec{k}\,(\neq\vec{q},\vec{0})}K(\vec{k},\vec{q})(\vec{k}\cdot\vec{q}/q^2)[S(|\vec{q}-\vec{k}|)-1] , \tag{3.6}$$

with

$$K(\vec{k},\vec{q})=\frac{\vec{q}\cdot\vec{k}}{k^2}+\frac{\vec{q}\cdot(\vec{q}-\vec{k})}{|\vec{q}-\vec{k}|^2} . \tag{3.7}$$

With these frequency moments, Eqs. (3.3) and (2.2b) yield the exact asymptotic behavior of the dielectric function:

$$\lim_{\omega\to\infty}\epsilon(q,\omega)=1-\frac{\omega_p^2}{\omega^2}-\frac{\omega_p^4}{\omega^4}\left[\frac{t_q^2}{\omega_p^2}+\frac{4\langle E_{\rm kin}\rangle t_q}{\hbar\omega_p^2}-I(q)\right]+\cdots . \tag{3.8}$$

On the other hand, if one adopts the *model* for the screened response function Eq. (2.5b), one finds for the $\omega^3$-sum rule (LF denotes local field)

$$\langle\omega^3\rangle_{\rm LF}=\frac{nq^2}{m}\left[t_q^2+4\langle E_{\rm kin}\rangle_0\frac{t_q}{\hbar}+\omega_p^2[1-G(q)]\right] , \tag{3.9a}$$

while the high-frequency expansion of $\epsilon(q,\omega)$ takes the form

$$\lim_{\omega\to\infty}\epsilon(q,\omega)=1-\frac{\omega_p^2}{\omega^2}-\frac{\omega_p^4}{\omega^4}\left[\frac{t_q^2}{\omega_p^2}+\frac{4\langle E_{\rm kin}\rangle_0 t_q}{\hbar\omega_p^2}-G(q)\right]+\cdots . \tag{3.9b}$$

Here, $\langle E_{\rm kin}\rangle_0=3\hbar^2q_F^2/10m$ is the kinetic energy per particle of a noninteracting system. On comparing Eqs. (3.5b) and (3.9a) we see that we may choose a local-field correction $G_3(q)$ which, when employed in Eq. (3.9a), will satisfy the $\omega^3$ sum rule, Eq. (3.5b); it is

$$G_3(q)=I(q)-\frac{2q^2}{m\omega_p^2}(\langle E_{\rm kin}\rangle-\langle E_{\rm kin}\rangle_0) . \tag{3.10}$$

Therefore, it is of interest to calculate $\langle E_{\rm kin}\rangle$ and to determine the function $I(q)$ from the Monte Carlo values for $S(q)$ through Eq. (3.6) in order to compare $G_3(q)$ with $G_0(q)$ in the Monte Carlo *plus* polarization potential model (MC + PPM).

In Table I we list the values of the relative difference in the kinetic energies,

$$\delta_K\equiv\langle E_{\rm kin}\rangle/\langle E_{\rm kin}\rangle_0-1 , \tag{3.11}$$

from the Monte Carlo results,[4,24] while in Appendix B we calculate this quantity in the high-density limit. With Eq. (3.11) one may rewrite Eq. (3.10) as

$$G_3(q)=I(q)-\frac{12}{5}\left[\frac{E_F^0}{\hbar\omega_p}\right]^2\delta_K\left[\frac{q}{q_F}\right]^2\simeq I(q)-\frac{2.713}{r_s}\delta_K\left[\frac{q}{q_F}\right]^2 . \tag{3.12}$$

The values of $I(q)$ which have been used in calculating $G_3(q)$ are also given in Table II, while in Fig. 4(a) we compare $G_3(q)$ and $G_0(q)$ for several values of $r_s$ and, in Fig. 4(b), compare $I(q)$ with four model calculations of $G(q)$. In Figs. 4(a) and 4(b) we have also indicated the values of $1-g(0)$ and $\frac{2}{3}[1-g(0)]$ from the Monte Carlo calculation of $g(r)$. Here, one should recall the limiting value of $G_0(q)$ [Eq. (2.26)], while Niklasson[20] has shown that, if one replaces $G(q)$ by a frequency-dependent function $G(q,\omega)$ in Eqs. (2.5a),

TABLE I. Mean kinetic energy per particle of an interacting system, $\langle E_{\rm kin}\rangle$, calculated from the ground-state energy per particle, $E_0/N$ (Ceperley and Alder, Ref. 4), and the mean potential energy per particle $\langle V_{\rm pot}\rangle$ (Ceperley, Ref. 24), for $r_s=1$, 2, 5, and 10. Also listed are the mean kinetic energy per particle for a noninteracting system, $\langle E_{\rm kin}\rangle_0=\frac{3}{5}E_F^0$, and the relative difference, $\delta_K\equiv\langle E_{\rm kin}\rangle/\langle E_{\rm kin}\rangle_0-1$. The energies are in units of rydbergs. The digits in parentheses indicate the error in the last decimal place of the Monte Carlo values.

| $r_s$ | $E_0/N$ | $\langle V_{\rm pot}\rangle$ | $\langle E_{\rm kin}\rangle$ | $\langle E_{\rm kin}\rangle_0$ | $\delta_K$ |
|---|---|---|---|---|---|
| 1 | 1.174(1) | −1.1157(8) | 2.290 | 2.2099 | 0.036 |
| 2 | 0.0041(4) | −0.5986(8) | 0.6027 | 0.552 47 | 0.091 |
| 5 | −0.1512(1) | −0.2654(1) | 0.1142 | 0.088 39 | 0.292 |
| 10 | −0.106 75(5) | −0.142 53(4) | 0.035 78 | 0.022 099 | 0.619 |

$$\lim_{q\to\infty} G(q,\omega)=\tfrac{2}{3}[1-g(0)]\ , \tag{3.13}$$

where we note that the function $I(q)$ has the same limit for large $q$.

From Figs 4(a) and 4(b), one observes the following.

(1) There is a large difference between $G_0(q)$ and $G_3(q)$ for all values of $r_s$ between 1 and 5. The value of $I(q)$ is about half of that of $G_0(q)$ for the same $r_s$. $I(q)$ and $G_0(q)$ become close only for very small values of $q$ ($\ll q_F$).

(2) $I(q)$ is a monotonically increasing function of $q$; there is no peak structure near $q=2q_F$ as found in $G_0(q)$ for $r_s=1$ and 2.

(3) For large values of $q$, where the second term on the right-hand side of Eq. (3.10) becomes appreciable, $G_3(q)$ takes on negative values.

(4) $G_0(q)$ approaches $1-g(0)$, whereas $I(q)$ goes to $\frac{2}{3}[1-g(0)]$ for large $q$.

Pathak and Vashishta[26] (PV) obtained a local-field

TABLE II. Function $I(q)$ [Eq. (3.6)] in the $\omega^3$ sum rule [Eq. (3.5b)] calculated from Ceperley's Monte Carlo data for the static form factor (Ref. 24).

| $q/q_F$ | $r_s=1$ | $r_s=2$ | $r_s=5$ |
|---|---|---|---|
| 0.125 | 0.0028 | 0.0030 | 0.0033 |
| 0.250 | 0.0110 | 0.0119 | 0.0133 |
| 0.375 | 0.0243 | 0.0263 | 0.0297 |
| 0.500 | 0.0421 | 0.0457 | 0.0518 |
| 0.625 | 0.0635 | 0.0693 | 0.0791 |
| 0.750 | 0.0876 | 0.0961 | 0.1105 |
| 0.875 | 0.1135 | 0.1252 | 0.1452 |
| 1.000 | 0.1404 | 0.1556 | 0.1821 |
| 1.125 | 0.1673 | 0.1864 | 0.2200 |
| 1.250 | 0.1937 | 0.2166 | 0.2580 |
| 1.375 | 0.2187 | 0.2457 | 0.2950 |
| 1.500 | 0.2421 | 0.2730 | 0.3302 |
| 1.625 | 0.2634 | 0.2981 | 0.3629 |
| 1.750 | 0.2825 | 0.3208 | 0.3926 |
| 1.875 | 0.2994 | 0.3410 | 0.4191 |
| 2.000 | 0.3142 | 0.3587 | 0.4425 |
| 2.125 | 0.3270 | 0.3743 | 0.4628 |
| 2.250 | 0.3382 | 0.3878 | 0.4805 |
| 2.375 | 0.3480 | 0.3996 | 0.4959 |
| 2.500 | 0.3566 | 0.4100 | 0.5092 |

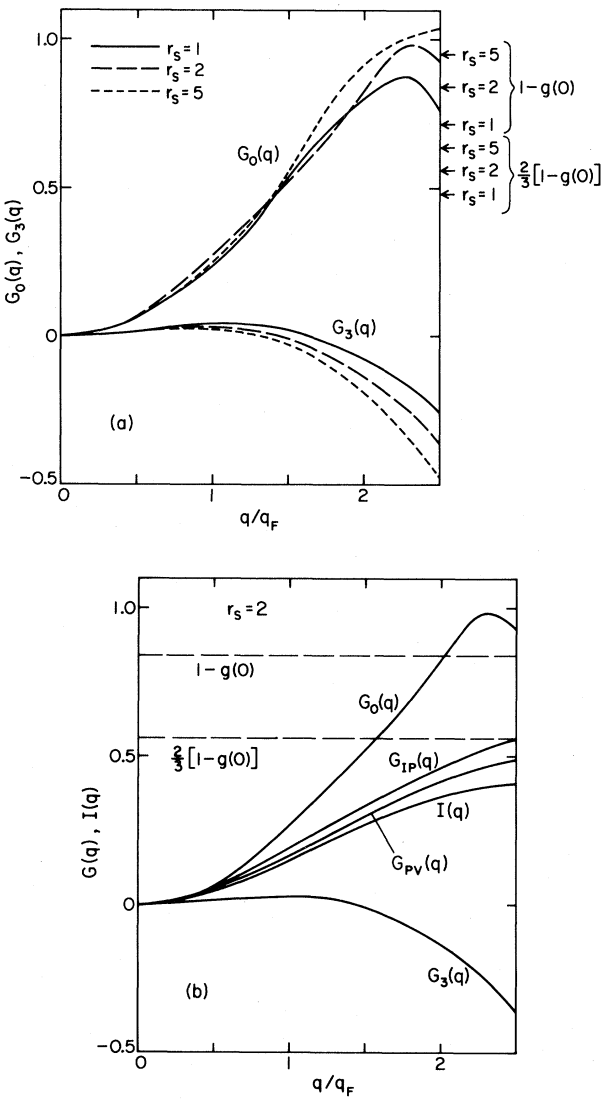


FIG. 4. (a) Comparison of local-field corrections $G_0(q)$ from Eq. (3.1) and $G_3(q)$ from the $\omega^3$-sum rule [Eq. (3.10)], for $r_s=1$, 2, and 5. Also shown are the values of $1-g(0)$ and $\frac{2}{3}[1-g(0)]$, where $g(0)$ is the Monte Carlo value of the pair correlation function at zero interparticle separation (Ref. 24). (b) Comparison of local-field corrections in different theories for $r_s=2$. The $G_0(q)$ is from Eq. (3.1); $G_{\rm IP}(q)$, from Ref. 1; $G_{\rm PV}(q)$, by Pathak and Vashishta (Ref. 26); and $G_3(q)$ from Eq. (3.10). The $I(q)$ is from Eq. (3.6). The values of $1-g(0)$ and $\frac{2}{3}[1-g(0)]$ are also shown.

correction $G_{PV}(q)$ and a static form factor which satisfy self-consistently both the $\omega^3$-sum rule and the fluctuation-dissipation theorem. However, in their calculation the difference between $\langle E_{kin}\rangle$ and $\langle E_{kin}\rangle_0$ was neglected, and $I(q)$ was treated as being identical to the local-field correction. As we have seen such a treatment is not justified: Even at small $r_s$ ($\sim 1$) a few percent relative difference between $\langle E_{kin}\rangle$ and $\langle E_{kin}\rangle_0$ causes a significant deviation of $G_3(q)$ from $I(q)$ at large $q$ ($\gg q_F$).

A proof that one cannot, with a static local-field correction, satisfy simultaneously the compressibility sum rule and the $\omega^3$-sum rule has been given by Vaishya and Gupta;[27] for a recent simple version of this proof, see Iwamoto.[28] The properties of the *dynamic* local-field correction have been studied by Kugler.[29]

The difference between $G_0(q)$, which was chosen to yield agreement with $S(q)$, and $G_3(q)$, which was chosen to yield agreement with the $\omega^3$-sum rule, furnishes a measure of the importance of multipair excitations. Because these lie, on the average, at greater energies than the single pair or plasmon energies, they make a much larger relative contribution to the $\omega^3$-sum rule than to $S(q)$. In the small-$q$ limit, their contribution to both quantities is of order $q^4$ (cf. Ref. 12), as is the contribution coming from $G(q)$.

In both of the above model calculations of $G(q)$, multipair excitations are not taken explicitly into account; in the MC + PPM approach, one distorts the local-field correction, and hence the pair plus plasmon spectrum, in such a way as to yield the correct $S(q)$, while with $G_3(q)$, one is distorting the pair plus plasmon spectrum in such a way as to obtain the correct value of $\langle\omega^3\rangle$. Since, as noted above, even in the long-wavelength limit, the contributions from multipair excitations to $S(q)$ and $\langle\omega^3\rangle$ are of the same order of magnitude as the modifications in the single pair plus plasmon part brought about by $G(q)$, the two calculations of $G(q)$ could not be expected to agree. Put another way, *neither* local-field correction is correct; the "true" local-field correction must be such as to allow room for multipair excitations [through an appropriate modification of $\chi(q,\omega)$] to contribute to both $S(q)$ and $\langle\omega^3\rangle$; it may be expected to lie between $G_0(q)$ and $G_3(q)$, as is the case for $G_{IP}(q)$.

In this connection, it is appropriate to refer to the study by Holas, Aravind, and Singwi,[30] who use perturbation theory to calculate the next higher-order terms beyond the RPA (the self-energy correction and the vertex correction to lowest-order proper polarization part). The resulting dielectric function involves a frequency-dependent local-field correction. However, it satisfies the $\omega^3$-sum rule only to lowest order, in that they find an expression of the form Eq. (3.8), in which $\langle E_{kin}\rangle$ is replaced by $\langle E_{kin}\rangle_0$, and $I(q)$ by its Hartree-Fock value.

## IV. STATIC FORM FACTOR AND CORRELATION ENERGY

For a given choice of $G(q)$, it is straightforward to calculate the static form factor $S(q)$ from Eqs. (2.6) and (2.9b). If, moreover, one knows the dependence of $G(q)$ upon $r_s$ it is likewise straightforward to calculate the contribution to the correlation energy arising from a given momentum transfer, and hence the overall correlation energy. In this section we give the results of such calculations for three different local-field corrections: $G_0(q)$, $G_{IP}(q)$, and the Hubbard local-field correction,

$$G_H(q)=\frac{2\pi e^2}{q^2+q_F^2}\ , \tag{4.1}$$

and compare them with the Monte Carlo results as well as with the RPA.

### A. Static form factor

Our calculation of $S(q)$ with Eq. (2.9b) and $G_0(q)$ serves as a test of the accuracy of the MSA, since the frequency integral in Eq. (2.9b) is carried out using the Lindhard function, $\chi_0(q,\omega)$, while the values of $G_0(q)$ were arrived at by making the MSA, and joining those results at small $q$ to $G_{IP}(q)$. We find the calculated values of $S(q)$ based on $G_0(q)$ agree to within 1% with the Monte Carlo (MC) result $S_{MC}(q)$ at the three densities ($r_s=1$, 2, and 5) studied. In Figs. 5(a)–5(c), we compare these results with $S_{IP}(q)$, the static structure factor calculated using $G_{IP}(q)$, and with $S_{RPA}(q)$, the RPA result [which correspond to $G(q)=0$]. We have also calculated $S_H(q)$, the static form factor using $G_H(q)$, [Eq. (4.1)], and find $S_H(q)\approx S_{IP}(q)$ for all values of $q$ and $r_s$ investigated.

We comment briefly on our results.

(1) For $q<0.6q_F$, we find $S_{IP}(q)\simeq S_{RPA}(q)\simeq S_{MC}(q)$; for these wave vectors plasmons at $\omega_p$ are the dominant excitation, and all three calculations are consistent with the exact long-wavelength result,

$$\lim_{q\to 0} S(q)=\frac{\hbar q^2}{2m\omega_p}\ . \tag{4.2}$$

(2) For $0.6q_F<q<q_F$, $S_{IP}(q)\simeq S_{MC}(q)$, while $S_{RPA}(q)$ is distinctly lower.

(3) For $q>q_F$, $S_{MC}(q)$ lies somewhat above $S_{IP}(q)$; as one goes to larger $r_s$, their relative difference increases, and is $\sim 8\%$ for $q\approx 2q_F$ and $r_s=5$. $S_{RPA}(q)$ continues to be lower than either for $q<2.5q$

(4) To the extent that $G_{IP}(q)$ provides an accurate account of local-field corrections within the framework of a more general theory which includes multipair excitations explicitly, the difference between $S_{IP}(q)$ and $S_{MC}(q)$ provides a direct measure of the contribution made by multipair excitations to $S(q)$.

In Fig. 6 we separate $S(q)$ into two contributions: a plasmon contribution and the single-pair plus multipair contributions. This figure illustrates how the plasmon contribution exhausts the total $S(q)$ at small $q$. Finally, we have made a numerical check of the $f$-sum rule by calculating

$$\frac{2m}{\hbar q^2}\int_0^\infty \frac{d\omega}{2\pi}\omega S(q,\omega)\ . \tag{4.3}$$

We found that this quantity is unity within 0.02% for $0\le q\le 2q_F$.

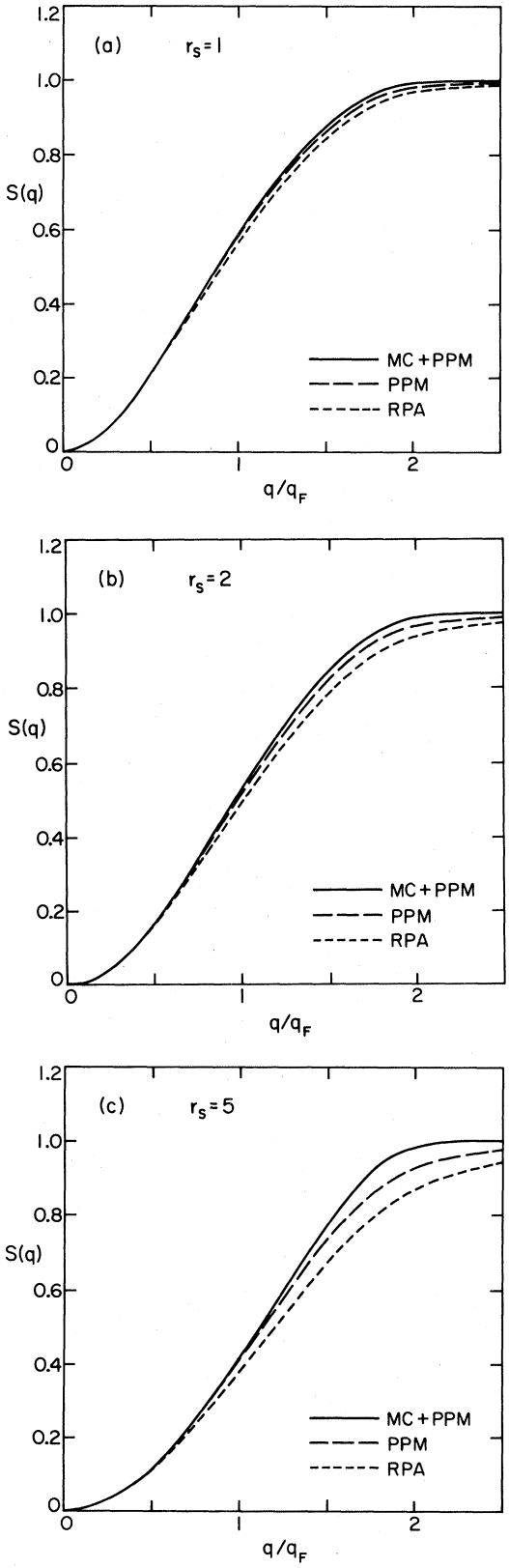


FIG. 5. (a) Comparison of the static form factors obtained from the three types of local-field corrections (MC + PPM, PPM, and RPA; see text) through the fluctuation-dissipation theorem for $r_s=1$. The initial Monte Carlo values for $S(q)$ are indistinguishably close to the curve MC + PPM. (b) Same as (a) for $r_s=2$. (c) Same as (a) for $r_s=5$.

### B. Correlation energy

The interaction energy in the ground state is defined as[12]

$$E_{\rm int}=\frac{n}{2}\sum_{\vec{q}}\frac{4\pi e^2}{q^2}[S(q)-1]\,. \tag{4.4}$$

Upon making use of the fluctuation-dissipation theorem [Eq. (2.8b)] and the definition of $S(q)$ [Eq. (2.9a)], one may write

$$E_{\rm int}=\sum_{\vec{q}}E_{\rm int}(q)=-\sum_{\vec{q}}\left[\hbar\int_0^\infty\frac{d\omega}{2\pi}{\rm Im}\frac{1}{\epsilon(q,\omega)}+\frac{2\pi ne^2}{q^2}\right]. \tag{4.5}$$

A theorem due to Pauli[12] allows one to write the ground-state energy as a sum of the free-particle kinetic energy and the coupling-constant integral of the interaction energy:

$$E_0=\tfrac{3}{5}N\left[\frac{\hbar^2q_F^2}{2m}\right]+\int_0^{e^2}\frac{d\lambda}{\lambda}E_{\rm int}(\lambda)\,, \tag{4.6}$$

where $E_{\rm int}(\lambda)$ is the interaction energy when the strength of the coupling constant is $\lambda$ rather than $e^2$. The correlation energy is defined as the difference between the true ground-state energy and the ground-state energy in the Hartree-Fock approximation. Thus from Eqs. (4.5) and (4.6),

$$E_{\rm corr}\equiv\int_0^\infty\frac{dq}{q_F}E_{\rm corr}(q) \tag{4.7a}$$

$$=-\sum_{\vec{q}}\int_0^{e^2}\frac{d\lambda}{\lambda}\hbar\int_0^\infty\frac{d\omega}{2\pi}{\rm Im}\left[\frac{1}{\epsilon(q,\omega;\lambda)}-\frac{1}{\epsilon_{\rm HF}(q,\omega;\lambda)}\right], \tag{4.7b}$$

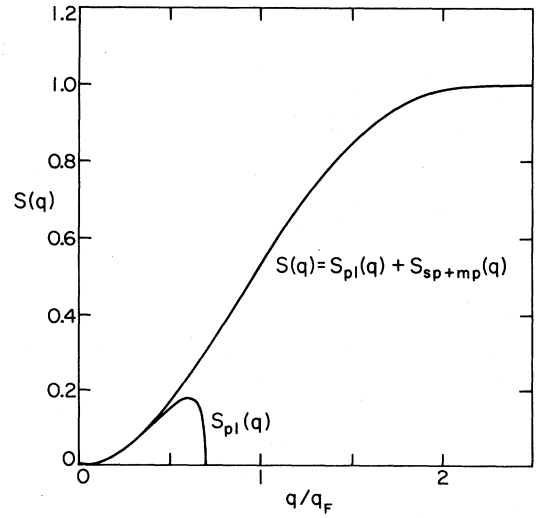


FIG. 6. Plasmon (pl) and the single-pair *plus* multipair (sp + mp) contributions to the static form factor for $r_s=2$.

where $\epsilon(q,\omega;\lambda)$ is the dielectric function with interaction strength $\lambda$, and $\epsilon_{\rm HF}(q,\omega;\lambda)$ is the dielectric function in the Hartree-Fock approximation [Eq. (2.3b)] when the coupling constant is $\lambda$ rather than $e^2$.

To perform the coupling-constant integration in Eq. (4.7b) we must, in principle, know the dependence of the local-field correction [or the effective interaction $v^s_{\rm eff}(q)$] on $r_s$. An interpolation formula for the density dependence of the parametrized pseudopotentials introduced in paper I is easily derived after which the coupling-constant integration may be carried out analytically. During our numerical investigations within that model, it turned out that it is sufficient to assume a density- (or $r_s$-) independent local-field correction, or, in other words, a pseudopotential which scales linearly with the coupling constant. The error introduced by this approximation was generally less than a percent of the correlation energy. In this approximation, we have simply

$$E_{\rm corr}=\sum_{\vec{q}}\hbar\int_0^\infty\frac{d\omega}{2\pi}\,{\rm Im}\left[\frac{1}{1-G(q)}\ln[1-v^s_{\rm eff}(q)\chi^0(q,\omega)]+\frac{4\pi e^2}{q^2}\chi^0(q,\omega)\right]. \tag{4.8}$$

It is convenient to normalize $E_{\rm corr}(q)$ by a factor $(2/\pi)\alpha r_s NE_F^0$ such that

$$\frac{E_{\rm corr}(q)}{(2/\pi)\alpha r_s NE_F^0}=\frac{1}{r_s}\int_0^{r_s}dr_s[S(q)-S_F(q)] \tag{4.9}$$

is dimensionless.[31]

We show the results for $E_{\rm corr}(q)$, the contributions to the correlation energy from different momentum transfers, in units of $(2/\pi)\alpha r_s NE_F^0$, in Figs. 7(a)–7(d). From these figures we see the following.

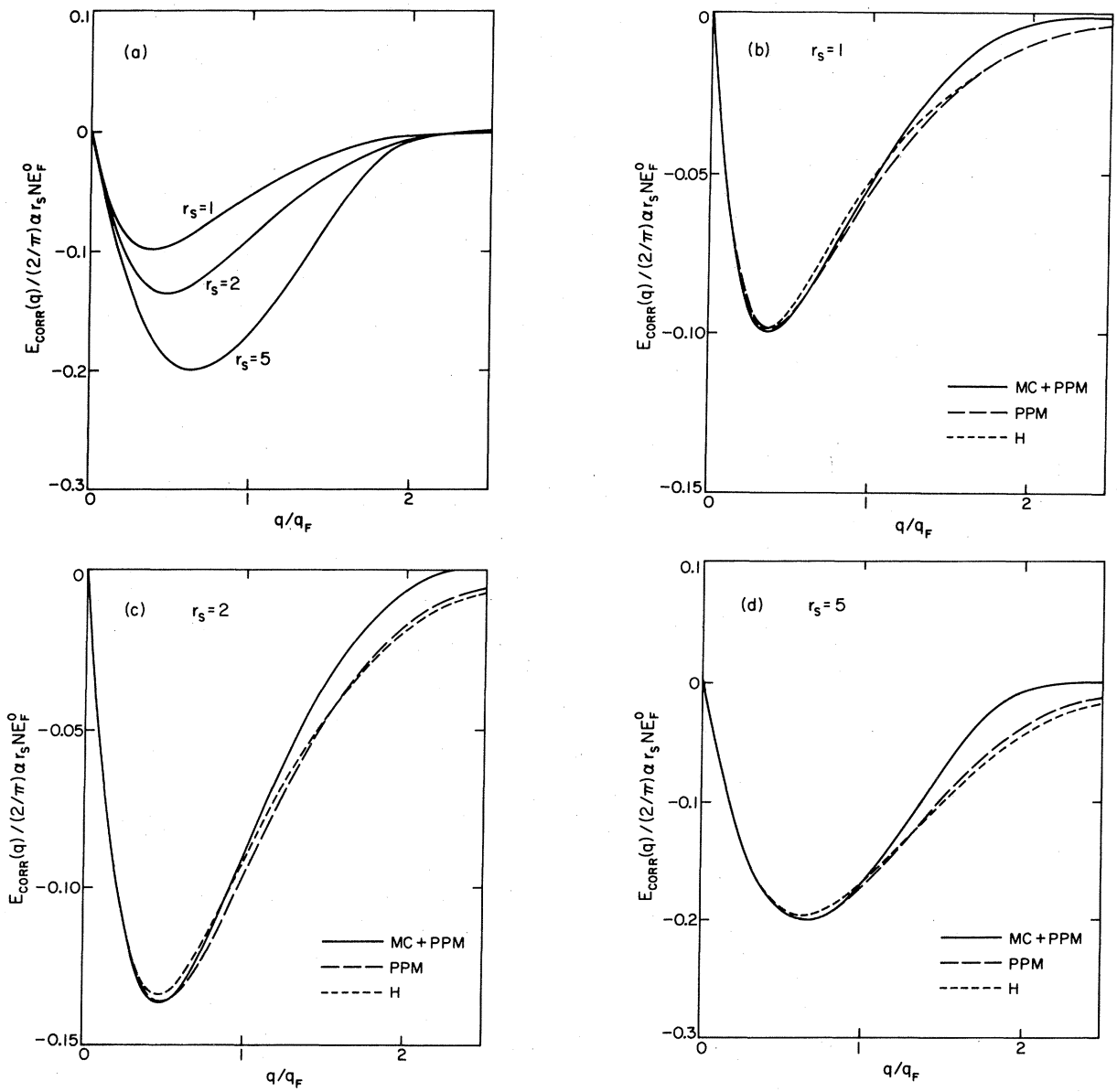


FIG. 7. Contributions to the correlation energy from different momentum transfers. (a) Monte Carlo *plus* polarization-potential model for $r_s=1$, 2, and 5. (b), (c), (d) Comparison of MC + PPM, PPM, and H for $r_s=1$, 2, and 5, respectively.

(1) $E_{\rm corr}(q)$ in these units decreases initially from 0 with increasing $q$ [one may easily verify from Eq. (4.8) that $E_{\rm corr}(q)$ starts in these units as $-S_F(q)$]. After reaching a minimum it heals back to 0 for $q \geq 2q_F$: Both magnitude and the location of the minimum increase for increasing $r_s$.

(2) The minima of $E^{\rm H}_{\rm corr}(q)$ (the Hubbard approximation) are shallower than those of $E^{\rm IKP}_{\rm corr}(q)$ (MC + PPM) (where IKP represents Iwamoto, Krotscheck, and Pines), while the former are slow in healing back to 0 for large $q$ ($\geq 3q_F$).

(3) $E^{\rm IP}_{\rm corr}(q)$ in the polarization-potential model is quite close to $E^{\rm IKP}_{\rm corr}(q)$ up to $q \approx q_F$ for $1 \leq r_s \leq 5$. As the was case for $S(q)$, we may attribute the difference between $E^{\rm IKP}_{\rm corr}(q)$ and $E^{\rm IP}_{\rm corr}(q)$ for $q > q_F$ to the role played by multipair excitations in determining $E_{\rm corr}(q)$, a role which is somewhat more pronounced as $r_s$ increases, and which is maximum for $q \approx 2q_F$.

(4) As was the case for $S(q)$, $E^{\rm IP}_{\rm corr}(q)$ is close to $E^{\rm H}_{\rm corr}(q)$ for all $q$: For $q \geq 2q_F$, the former is slightly above the latter.

Finally, we integrate $E_{\rm corr}(q)$ in our Monte Carlo *plus* polarization-potential model to obtain the correlation energy and compare it with the original Monte Carlo data. We find that in our model $E_{\rm corr}/N$ reproduces, within the accuracy of the present numerical calculation (0.3%, 0.8%, and 1.2% for $r_s = 1$, 2, and 5, respectively), the original Monte Carlo correlation energy.

## V. PLASMON DISPERSION AND DYNAMIC FORM FACTOR

In this section we present the results of our calculations of plasmon dispersion and the dynamic form factor using the local-field corrections $G_0(q)$ (Monte Carlo plus polarization-potential model), $G_{\rm IP}(q)$ (polarization-potential model), and $G_{\rm H}(q)$ (Hubbard approximation), and compare these results with the RPA and with experiment.

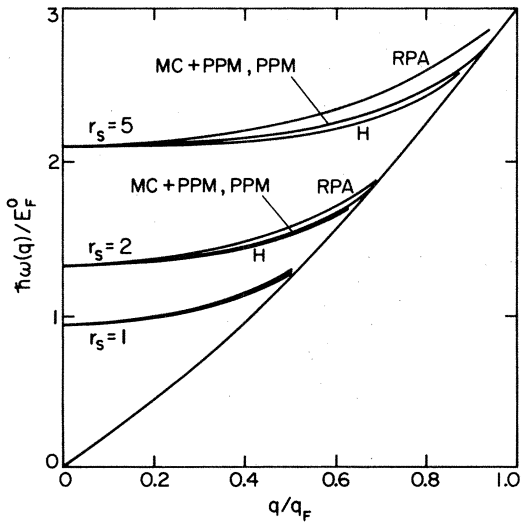


FIG. 8. Plasmon dispersion obtained from the four different local-field corrections (MC + PPM, PPM, H, and RPA) for $r_s = 1$, 2, and 5 (see text).

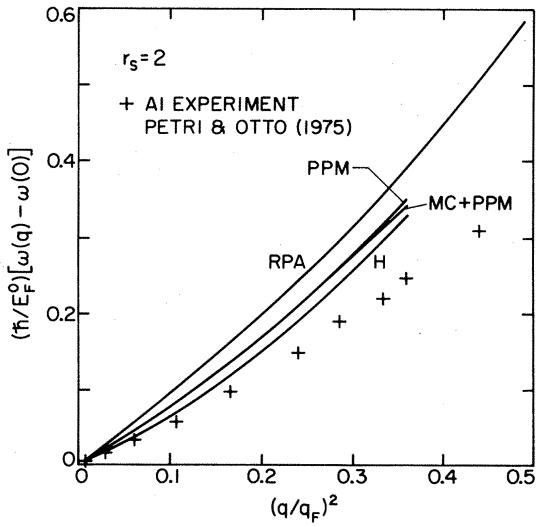


FIG. 9. Plot of $\omega(q) - \omega(0)$ in units of $E_F^0/\hbar$ vs $(q/q_F)^2$. The four curves result from MC + PPM, PPM, H, and RPA. The crosses show experimental data due to Petri and Otto [Ref. 32 for Al ($r_s = 2.07$)].

### A. Plasmon dispersion

The plasmon-dispersion relation $\omega = \omega(q)$ is given by the solution of the equation

$$\epsilon(q, \omega(q)) = 0 \, . \tag{5.1}$$

Our results are shown in Fig. 8. One sees that the three models for $G(q)$ give almost indistinguishable plasmon-dispersion curves for $r_s = 1$ and 2. For $r_s = 5$, the MC + PPM and PPM results are close, while that based on $G_{\rm H}(q)$ starts to deviate from these two curves at $q \approx 0.2q_F$ before it finally merges into the single-pair continuum at $q \approx 0.92q_F$. The RPA curve always lies above those with nonvanishing $G(q)$.

We show the quantity $\omega(q) - \omega(0)$ as a function of $q^2$ in Figs. 9 and 10 for $r_s = 2$ and 5, respectively. In these fig-

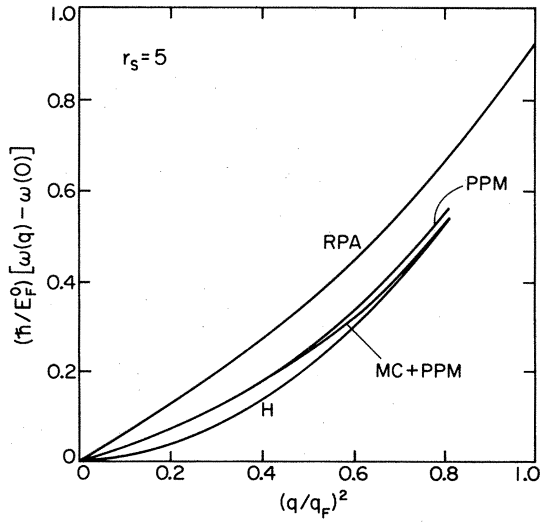


FIG. 10. Same as Fig. 9 for $r_s = 5$.

ures we also include the RPA results as well as the experimental values for Al ($r_s=2.07$) by Petri and Otto.[32] The agreement is poor: The experimental points do not lie on any of the theoretical curves (see Sec. V B).

### B. Plasmon-dispersion coefficient

In comparing the theoretical plasmon dispersion with experiment it is useful to introduce the *plasmon-dispersion coefficient:*

$$\alpha=\frac{m}{\hbar}\frac{\partial^2\omega(q)}{\partial q^2}\bigg|_{q=0} . \tag{5.2}$$

Strum[33] suggests that one use the portion of the plasmon dispersion for which $(q/q_F)^2<1$. His reasoning is that for such wave numbers the plasmon dispersion is well described as being quadratic in $q$,

$$\omega(q)=\omega_p+\frac{\hbar}{m}\alpha q^2 , \tag{5.3}$$

in the RPA. However, such a restricted wave-number region makes it difficult to extract the dispersion coefficient from experiment, especially for the alkali metals (Li, Na, and K). For Al, on the other hand, Möller and Otto[34] suggest using the large-wave-number portion of the experimental plasmon dispersion, since the influence of the low-lying interband transitions is pronounced in the small-wave-number region. On modifying the definition of $\alpha$ to

$$\alpha_{\rm H}\equiv\frac{m}{\hbar}\frac{\partial^2\omega(q)}{\partial q^2}\bigg|_{q=\tilde{q}} , \tag{5.4}$$

with $\tilde{q}=0.8q_c$ ($q_c$ being the cutoff wave number at which the plasmon-dispersion curve merges into the continuum), they find good agreement between theoretical and experimental values of $\alpha_{\rm H}$. In Figs. 11 and 12 we plot the wave-number-dependent plasmon-dispersion coefficient,

$$\alpha(q)=\frac{m}{\hbar q^2}[\omega(q)-\omega(0)] , \tag{5.5}$$

for $r_s=2$ and 5. This quantity is related to the quantity $\alpha$ introduced in Eq. (5.2) by

$$\alpha(q=0)=\alpha . \tag{5.6}$$

Several experimental values for Al ($r_s=2.07$) and K ($r_s=4.86$) are also shown for comparison with the theoretical values for $\alpha(q=0)$.

In the case of Al the comparison with experiment is not straightforward. The plasmon-dispersion coefficient in Al has been measured experimentally to have two different values for $q<0.3q_F$ and $q>0.3q_F$.[32,34,39,40] In both wave-number regions, the dispersion is well described by a quadratic dependence on $q$. In the small-wave-number region ($q<0.3q_F$), $\alpha(q)\approx 0.2$, while in the large-wave-number region ($q>0.3q_F$), $\alpha(q)\approx 0.4$. In comparing theoretical values for $\alpha(q)$ with experiment, the small-wave-number region seems appropriate, since the small-wave-number expansion is used to obtain the theoretical values. On the other hand, the solid-state effects due to low-lying interband transitions are expected to modify the plasmon dispersion in such a region.[34,39] As for the large-wave-number region, where such effects are expected to be small, the higher-order terms in the expansion are no longer negligible.[33] For K, the theoretical values based on both $G_0(q)$ and $G_{\rm IP}(q)$ are in good agreement with experiment.

### C. Dynamic form factor

The dynamic form factor $S(q,\omega)$ may be calculated from Eqs. (2.5b) and (2.8a). We show the results of our model calculations of $S(q,\omega)$ based on $G_0(q)$, $G_{\rm IP}(q)$, and

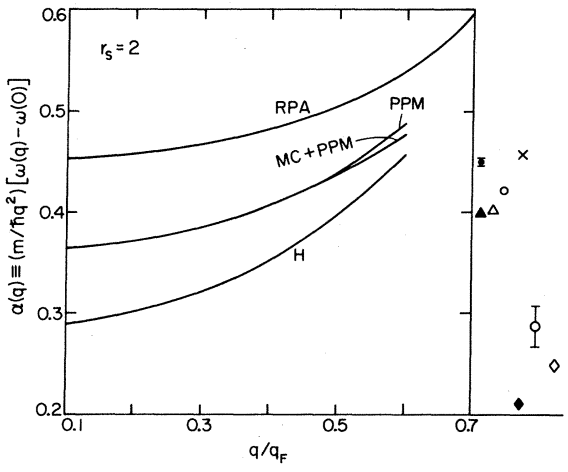


FIG. 11. Wave-number-dependent plasmon dispersion coefficient [Eq. (5.5)] for $r_s=2$. Four theoretical curves (MC + PPM, PPM, H, and RPA) as well as experimental values for Al ($r_s=2.07$) at $q=0$ [$\alpha(0)$] are shown. Experimental results are due to Sueoka (Ref. 35, open diamond), Kunz (Ref. 38, open circle with error bar), Kloos (Ref. 39 solid circle with error bar), Höhberger, Otto, and Petri (Ref. 36, open triangle), Petri and Otto (Ref. 32, solid triangle), Gibbons *et al.* (Ref. 37, open circle without error bar), and Krane (Ref. 40; cross for high $q$, solid diamond for low $q$).

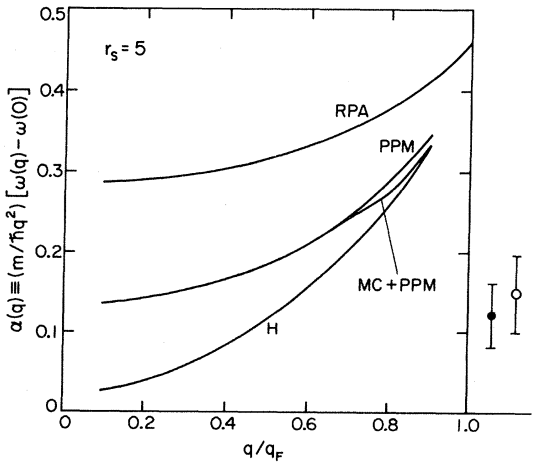


FIG. 12. Same as Fig. 11 for $r_s=5$. Experimental results for K ($r_s=4.86$) are due to Kunz (Ref. 38, open circle) and Kloos (Ref. 39, solid circle).

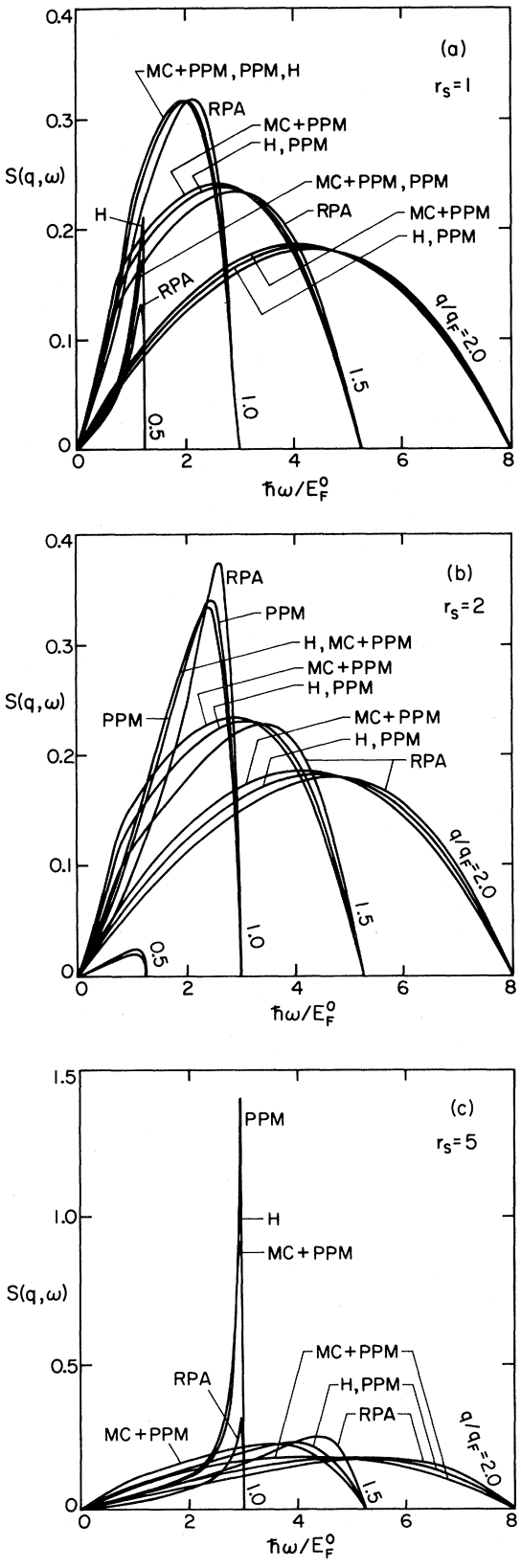


FIG. 13. (a) Dynamic form factors calculated from different $G(q)$'s (MC + PPM, PPM, H, and RPA) at several values of momentum transfer ($q/q_F=0.5$, 1, 1.5, and 2) for $r_s=1$. (b) Same as (a) for $r_s=2$. (c) Same as (a) for $r_s=5$.

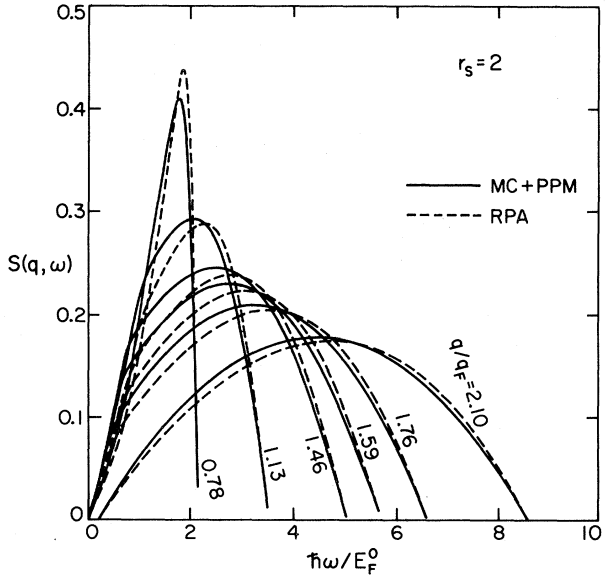


FIG. 14. Dynamic form factor calculated from $G(q)$ in the Monte Carlo *plus* polarization-potential model at several values of momentum transfer ($q/q_F=0.78$, 1.13, 1.46, 1.59, 1.76, and 2.10) for $r_s=2$.

$G_H(q)$ at different wave numbers ($q/q_F=0.5$, 1, 1.5, and 2) for $r_s=1$, 2, and 5 in Figs. 13(a), 13(b), and 13(c), respectively. We observe that for a given momentum transfer, the peak positions of $S(q,\omega)$ in these four models (MC + PPM, PPM, H, and RPA) are slightly different. The peak of $S(q,\omega)$ in the RPA lies at the largest energy transfer; those of H, PPM, and MC + PPM occur at lower values of energy transfer, in this order.

The dynamic form factor has been measured in x-ray scattering experiments for Be,[41–43] graphite,[43] Al,[43] and Li.[44] We compare our theoretical curves (MC + PPM) for $r_s=2$ (Fig. 14) with experiment for Be ($r_s=1.86$) (Fig. 15)

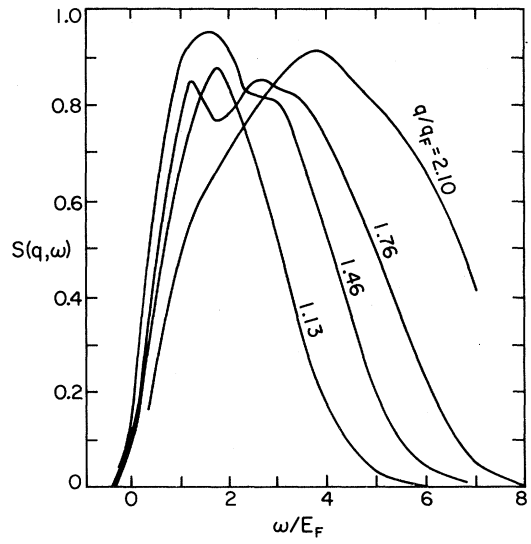


FIG. 15. Unnormalized dynamic form factor for Be ($r_s=1.86$) measured in an inelastic x-ray scattering experiment by Platzman and Eisenberger (Ref. 43).

(Ref. 43) for several values of momentum transfer. We observe the following.

(1) None of the theoretical curves contain the double-peak structure which is found experimentally for $q/q_F = 1.46$ and 1.76. It would seem physically reasonable to attribute this double-peak structure to the multipair excitations, since we have argued that these begin to play an important role for $q > q_F$, and since, moreover, such excitations are known to play an important role at such wave vectors for $^3$He.[6] This explanation is consonant with two others which have recently been put forward: The influence of the dynamic screening[45] and the nonanalytical structure of the self-energy,[46,47] since each of these represents a specific way of incorporating explicitly the contribution of multipair excitations to $S(q,\omega)$. Because no explicit contribution of multipair excitations is included in the response function, Eq. (2.5b), it is scarcely surprising that a double-peak structure is not found for $S(q,\omega)$.

(2) As mentioned earlier, the peak positions of $S(q,\omega)$ in MC + PPM are shifted towards lower values of energy transfer ($\hbar\omega/E_F^0$) compared with those in the RPA. However, the peaks in the experimental curves occur at still lower values of energy transfer. Green, Lowy, and Szymanski[45] suggest that, due to a systematic error in the $\omega$ calibration in the experiment, the experimental peaks may appear to be lower than they actually are.

## VI. DISCUSSION

We have seen that to the extent that the density-density response function may be written in the form Eq. (2.5b), once one adopts an expression for $G(q)$ it is straightforward to calculate $S(q)$ by using the fluctuation-dissipation theorem, Eq. (2.9b). If one has, moreover, a second relation between $G(q)$ and $S(q)$, one can carry out a self-consistent calculation of $G(q)$.[48] The first attempt at such a self-consistent calculation was the theory of Singwi *et al.*[49]; in their theory, the Bogoliubov-Born-Green-Kirkwood-Yvon (BBGKY) equations were truncated by assuming a form for the two-particle correlation function, which led to a dielectric function of a form similar to Eq. (2.2a) with Eq. (2.5a), and $G(q)$ is given as a functional of $S(q)$. On the other hand, Pathak and Vashishta[26] used the $\omega^3$-sum rule to establish a relation between $G(q)$ and $S(q)$ [Eq. (3.6) in which $I(q)$ is regarded as being identical to $G(q)$]. The calculation of $G_0(q)$ presented in Sec. III may likewise be classified as a self-consistent one, since the mean spherical approximation [Eqs. (2.18) and (2.20)] provides the necessary relations between $S(q)$ and $G(q)$, and $S^a(q)$ and $G^a(q)$. However, it differs from the previous theories in several ways. We list the characteristic differences.

(1) Self-consistency: $G_0(q)$, obtained by Eq. (3.1) from the Monte Carlo data for $S(q)$, reproduces the initial input $S(q)$ through the fluctuation-dissipation theorem [Eq. (2.9b)] within errors of less than 1%. We note that the use of the MSA in our calculation is merely a matter of convenience in numerical calculations.

(2) Compressibility sum rule and the static spin susceptibility: In the long-wavelength region, where the available Monte Carlo data have substantial error bars, the polarization-potential model developed in paper I was used to obtain $G(q)$ and $G^a(q)$. This guarantees the long-wavelength behavior of the dielectric function and the static spin susceptibility function. The dielectric function satisfies the compressibility sum rule exactly, while the spin susceptibility has a correct long-wavelength behavior. In other words, the long-wavelength limits of the dielectric function and the spin susceptibility function are adjusted to the compressibility and the static spin susceptibility calculated from the Monte Carlo data for the spin-dependent correlation energy.

(3) Positivity of the pair correlation function $g(r)$: The Monte Carlo method allows one to calculate $g(r)$ directly; $g(r)$ is then used to obtain $S(q)$. The problem of negative $g(r)$ does not exist.

We have already noted that $G_0(q)$ differs significantly from the function $G_3(q)$, which is constructed so that the calculated $S(q,\omega)$ will satisfy the $\omega^3$-sum rule. These functions should be identical if the form (2.5a) were exact. We argue that the numerical values for the function $I(q)$ we have obtained [Table II and Fig. 4(b)] are quite accurate in the light of the reliability of the Monte Carlo data for $S(q)$. Thus $G_3(q)$ from these values of $I(q)$ in Eq. (3.10), if it is used in place of $G_0(q)$ to calculate $S(q)$, cannot reproduce the Monte Carlo $S(q)$. We conclude therefore that the inconsistency stems from the form of the screened response function [Eq. (2.5a)]. In other words, as long as one adopts Eq. (2.5a) as a form of the screened response function, such an inconsistency is unavoidable. One obvious reason is the use of the *static* local-field correction in Eq. (2.5a); i.e., to obtain a theory which yields both $S(q)$ and satisfies the $\omega^3$-sum rule, it is essential that one take multipair excitations explicitly into account.

By comparing the results of calculations based on $G_{\rm IP}(q)$ with the Monte Carlo results for $S(q)$ and $E_{\rm corr}(q)$, we conclude that for $q < q_F$, multipair excitations do not make an appreciable contribution to either of these quantities (nor is their contributin to $\langle\omega^3\rangle$ substantive). On the other hand, for $q_F < q < 2.5q_F$, it is important to take them into account explicitly in $\chi(q,\omega)$, since only in that way can one hope to carry out consistent calculations of $S(q)$ and $\langle\omega^3\rangle$, as well as to obtain the observed double-peak structure of $S(q,\omega)$.

There is an interesting object lesson to be learned from our calculations based on $G_0(q)$. Although we are able to calculate correctly $S(q)$ and $E_{\rm corr}(q)$, to satisfy the $f$-sum rule, and to obtain good agreement with experiment for plasmon dispersion, the response function, Eq. (2.5b), is *not* the correct one—as one finds out when one either compares theory with experiment for $S(q,\omega)$ or examines the $\langle\omega^3\rangle$-sum rule. In the next planned paper in this series we discuss phenomenological expression for $\chi(q,\omega)$ which do not suffer from this defect. We shall discuss the extent to which one can construct a $\chi(q,\omega)$ which satisfies the $f$-sum rule, yields both $S(q)$ and $\langle\omega^3\rangle$, and leads to a two-peak structure for $S(q,\omega)$.

We have focused our attention in this paper on calculations of $G(q)$ and of $S(q,\omega)$; thus after presenting our results for $G_0^a(q)$, we do not attempt an analysis of their ac-

curacy. If, following Goodman and Sjölander,[50] one considers the $\omega^3$-sum rule for the spin-fluctuation spectral density, $S^a(q,\omega)$, one finds that it is impossible to satisfy this sum rule with $G_0^a(q)$. The physical reason for this discrepancy is, again, the role played by multipair excitations. As noted by Goodman and Sjölander, multipair excitations play an even more important role in $S^a(q,\omega)$, since these contribute terms of order $q^2$ in all the relevant sum rules.

In summary, we have examined the consequences of the screened response function (2.5a) by making full use of the reliable Monte Carlo data. In a sense we have established a beginning for a new generation of many-body theories, which take full advantage of the possibility today of performing virtually exact computation of ground-state properties, and utilize the input from those computations in studies of excited states.

## ACKNOWLEDGMENTS

This work was supported in part by the National Science Foundation under Grants Nos. PHY-77-27084 (supplemented by funds from the U. S. National Aeronautics and Space Administration), PHY-80-25605, and DMR-82-15128 and for one of us (E.K.) by the Deutsche Forschungsgemeinschaft through a Heisenberg Fellowship. This work was initiated and completed at the Aspen Center for Physics and it gives us pleasure to thank the Center for its hospitality.

## APPENDIX A: MEAN SPHERICAL APPROXIMATION

In this appendix we describe the "mean spherical approximation" (MSA) and derive the expression for the static form factor within this approximation. The MSA amounts to the replacement of the hole-state sum of the single-particle propagator by a judiciously weighted collective propagator. In a formal representation, one may phrase the MSA in the form of Ref. 11,

$$\left\langle \frac{1}{e} \right\rangle \approx \frac{1}{\langle e \rangle} . \tag{A1}$$

where the average $\langle \cdots \rangle$ of a function of a particle and a hole momentum $f(\vec{p},\vec{h})$ is defined as

$$\langle f(\vec{p},\vec{h}) \rangle(q) \equiv \frac{\sum_{\vec{h}} \Theta(q_F - |\vec{h}|)\Theta(|\vec{h}+\vec{q}| - q_F) f(\vec{h}+\vec{q},\vec{h})}{\sum_{\vec{h}} \Theta(q_F - |\vec{h}|)\Theta(|\vec{h}-\vec{q}| - q_F)} . \tag{A2}$$

In the approximation (A2) the free-electron-gas response function $\chi^0(q,\omega)$ reduces to the simple form

$$\chi^0_{\mathrm{MSA}} = \frac{nq^2/2m}{\omega^2 - [\hbar q^2/2mS_F(q)]^2} , \tag{A3}$$

i.e., the single pair continuum is approximated by a collective mode with an energy $\hbar^2 q^2/2mS_F(q)$.

In other words, the MSA is equivalent to making the free fermion equivalent of the Feynman calculation of the excitation spectrum of $^4$He, in that one assumes that a single collective mode, of frequency

$$\Omega_q = \hbar q^2/2mS(q) \tag{A4}$$

exhausts the $f$-sum rule and yields the static structure factor in suitable approximation. Thus for a noninteracting electron gas, one has

$$S^0_{\mathrm{MSA}}(q,\omega) = 2\pi S_F(q)\delta(\omega - \Omega_q^F) , \tag{A5}$$

where

$$\Omega_q^F = \hbar q^2/2mS_F(q) , \tag{A6}$$

a result equivalent to Eq. (A3).

For the interacting electron liquid, in the local-field approximation, application of the MSA yields

$$S_{\mathrm{MSA}}(q,\omega) = 2\pi S(q)\delta(\omega - \Omega_q) , \tag{A7}$$

where

$$\Omega_q = \left[ \frac{nq^2 v^s_{\mathrm{eff}}(q)}{m} + (\Omega_q^F)^2 \right] \equiv \{\omega_p^2[1-G(q)] + [\hbar q^2/2mS_F(q)]^2\}^{1/2} . \tag{A8}$$

and $S(q)$ is given by Eq. (2.18). The corresponding expression for $\chi(q,\omega)$ is

$$\chi_{\mathrm{MSA}}(q,\omega) = \frac{nq^2/2m}{\omega^2 - [\hbar q^2/2mS_F(q)]^2 - (nq^2/m)v^s_{\mathrm{eff}}(q)} \tag{A9}$$

It should be obvious that the form (A9) for the response function is adequate only if a subsequent frequency integral is performed. To find the local-field correction such that one obtains the correct static form factor, one simply equates Eq. (A8) with Eq. (A4); the resulting "best" local-field correction is then

$$G_0(q) = 1 + \frac{\hbar^2 q^4}{4m^2\omega_p^2} \left[ \frac{1}{[S_F(q)]^2} - \frac{1}{[S(q)]^2} \right] , \tag{A10}$$

from which Eq. (3.1) directly follows.

## APPENDIX B: KINETIC ENERGY OF AN INTERACTING ELECTRON GAS IN THE HIGH-DENSITY LIMIT

In this appendix we calculate the kinetic energy per particle of an interacting electron gas at high densities. For small $r_s$, the ground-state energy per particle of an electron gas in Ry has been calculated to be[51–55]

$$\frac{E_0}{N}=\frac{3}{5}\frac{1}{\alpha^2 r_s^2}-\frac{3}{2\pi}\frac{1}{\alpha r_s}+\frac{2}{\pi^2}(1-\ln 2)\ln r_s -0.094-0.013 r_s\ln r_s+O(r_s) \tag{B1a}$$

$$=\frac{2.2099}{r_s^2}-\frac{0.9163}{r_s}+0.062\,18\ln r_s -0.094-0.013 r_s\ln r_s+O(r_s)\,. \tag{B1b}$$

The use of the virial theorem gives the kinetic energy per particle as[56–58]

$$\langle E_{\rm kin}\rangle=-\frac{d}{dr_s}\left[r_s\left[\frac{E_0}{N}\right]\right]\,. \tag{B2}$$

From Eqs. (B1) and (B2) one obtains

$$\langle E_{\rm kin}\rangle=\frac{2.2099}{r_s^2}+0.032-0.062\,18\ln r_s +0.026 r_s\ln r_s+0.013 r_s+O(r_s) \tag{B3}$$

in Ry. The first term on the right-hand side of Eq. (B3) is the kinetic energy per particle of a noninteracting electron gas. Thus the relative difference of the kinetic energies [Eq. (3.11)] is

$$\delta_K=0.014 r_s^2-0.028\,14 r_s^2\ln r_s+0.012 r_s^3\ln r_s +0.0059 r_s^3+O(r_s^3), \tag{B4}$$

where the last term on the right-hand side of Eq. (B4) indicates the uncertainty in terms of the $r_s$ parameter due to the lack of calculation of the ground-state energy to order $r_s$ [Eq. (B1)]. Neglecting this term one can evaluate $\delta_K$ to be $1.4\times10^{-5}$ ($r_s=0.01$), $7.7\times10^{-4}$ ($r_s=0.1$), and $8.1\times10^{-3}$ ($r_s=0.5$), while for $r_s=1$, one has, from Table I, $\delta_K=3.6\times10^{-2}$. By keeping the first two terms on the right-hand side of Eq. (B4), Eq. (3.12) becomes

$$G_3(q)\simeq I(q)-(0.038-0.076\ln r_s)r_s(q/q_F)^2\,. \tag{B5}$$

This expression demonstrates the limiting behavior $G_3(q)\to I(q)$ as $r_s\to0$.

---

*Present address: Department of Physics, Washington University, St. Louis MO 63130.

†Present address: Max Planck Institut für Kernphysik, Postfach 103980 Heidelberg, Germany.

[1]N. Iwamoto and D. Pines, this issue, preceding paper, Phys. Rev. B 29, 3924 (1984) (paper I, hereafter referred to as IP).

[2]N. Iwamoto, E. Krotscheck, and D. Pines, paper III (unpublished).

[3]N. Iwamoto, E. Krotscheck, and D. Pines, paper IV (unpublished).

[4]D. M. Ceperley and B. J. Alder, Phys. Rev. Lett. 45, 566 (1980).

[5]S. H. Vosko, L. Wilk, and M. Nusair, Can. J. Phys. 58, 1200 (1980).

[6]C. H. Aldrich III and D. Pines, J. Low Temp. Phys. 32, 689 (1978); for a review, see D. Pines, in Proceedings of the LXXXIX Varenna School on "Highlights of Condensed Matter Theory" (in press).

[7]E. Krotscheck and M. L. Ristig, Phys. Lett. A 48, 17 (1974).

[8]E. Feenberg, *Theory of Quantum Fluids* (Academic, New York, 1969).

[9]E. Krotscheck, Phys. Rev. A 26, 3536 (1982).

[10]E. Krotscheck, Ann. Phys. (N.Y.) (to be published).

[11]R. F. Bishop and K. H. Lührmann, Phys. Rev. B 26, 5523 (1982).

[12]D. Pines and P. Nozières, *The Theory of Quantum Liquids* (Benjamin, New York, 1966), Vol. I.

[13]We define the dynamic form factor $S(q,\omega)$ such that the frequency integral of it gives the static form factor $S(q)$ [Eq. (2.9a)]. Therefore, the relation to the notation in Ref. 12 is $S(q,\omega)=(2\pi/n)S^{\rm PN}(q,\omega)$.

[14]G. Ripka, Phys. Rep. 56, 1 (1979).

[15]J. G. Zabolitzky, Phys. Rev. B 22, 2353 (1980).

[16]One way to obtain Eq. (2.18) is to take the high-density limit of the quasiboson approximation (Ref. 15) or the FHNC theory (Ref. 10). Then, Eq. (2.18) with $v_{\rm eff}(q)$ replaced by $v(q)$, the bare Coulomb potential, is obtained:

$$S(q)=\frac{S_F(q)}{\{1+(4mn/\hbar^2q^2)v(q)[S_F(q)]^2\}^{1/2}}\,.$$

The correlation energy calculated from this expression differs from the correct value by 8.3% in the high-density limit.

[17]E. Krotscheck, in Proceedings of the Symposium on Quantum Fluids and Solids, Sanibel, Florida (AIP, New York, in press).

[18]J. C. Kimball, Phys. Rev. A 7, 1648 (1973).

[19]R. W. Shaw, Jr., J. Phys. C 3, 1140 (1970).

[20]G. Niklasson, Phys. Rev. B 10, 3052 (1974).

[21]J. Hubbard, Proc. R. Soc. London, Ser. A 243, 336 (1957).

[22]See the following reviews: K. S. Singwi and M. P. Tosi, in *Solid State Physics*, edited by H. Ehrenreich, F. Seitz, and D. Turnbull (Academic, New York, 1981), Vol. 36, p. 177; S. Ichimaru, Rev. Mod. Phys. 54, 1017 (1982).

[23]D. Ceperley, Phys. Rev. B 18, 3126 (1978).

[24]D. Ceperley (private communcation).

[25]R. D. Puff, Phys. Rev. 137, A406 (1965); N. Mihara and R. D. Puff, Phys. Rev. 174, 221 (1968).

[26]K. N. Pathak and P. Vashishta, Phys. Rev. B 7, 3649 (1973).

[27]J. S. Vaishya and A. K. Gupta, Phys. Rev. B 7, 4300 (1973).

[28]N. Iwamoto, Institute for Theoretical Physics (Santa Barbara) Report No. NSF-ITP-83-127 (unpublished).

[29]A. A. Kugler, J. Stat. Phys. 12, 35 (1975).

[30]A. Holas, P. K. Aravind, and K. S. Singwi, Phys. Rev. B 20, 4912 (1979).

[31]Often in the scientific literature (cf. Refs. 12 and 21), $E_{\rm corr}(q)$ is normalized by a factor $(3/4\pi)NE_F^0$ such that

$$\frac{E_{\rm corr}(q)}{(3/4\pi)NE_F^0}$$

$$= -x^2 \int_0^{e^2} \frac{d\lambda}{\lambda} \int_0^{\infty} dy \, \mathrm{Im} \left[ \frac{1}{\epsilon(q,\omega,\lambda)} - \frac{1}{\epsilon_{\rm HF}(q,\omega;\lambda)} \right],$$

which is also dimensionless. Here $x=q/q_F$ and $y=\hbar\omega/E_F^0$.


[32]E. Petri and A. Otto, Phys. Rev. Lett. 34, 1283 (1975).

[33]K. Sturm, Solid State Commun. 27, 645 (1978); Phys. Rev. Lett. 46, 1706(C) (1981).

[34]H. Möller and A. Otto, Phys. Rev. Lett. 45, 2140 (1980); 46, 789(E) (1981); 46, 1707(C) (1981).

[35]O. Sueoka, J. Phys. Soc. Jpn. 20, 2249 (1965).

[36]H. J. Höhberger, A. Otto, and E. Petri, Solid State Commun. 16, 175 (1975).

[37]P. C. Gibbons, S. E. Schnatterly, J. J. Ritsko, and J. R. Fields, Phys. Rev. B 13, 2451 (1976).

[38]C. Kunz, Z. Phys. 196, 311 (1966).

[39]T. Kloos, Z. Phys. 265, 225 (1973).

[40]K. J. Krane, J. Phys. F 8, 2133 (1978).

[41]P. Eisenberger, P. M. Platzman, and K. C. Pandy, Phys. Rev. Lett. 31, 311 (1973).

[42]P. M. Platzman and P. Eisenberger, Solid State Commun. 14, 1 (1974).

[43]P. M. Platzman and P. Eisenberger, Phys. Rev. Lett. 33, 152 (1974).

[44]P. Eisenberger, P. M. Platzman, and P. Schmidt, Phys. Rev. Lett. 34, 18 (1975).

[45]F. Green, D. N. Lowy, and J. Szymanski, Phys. Rev. Lett. 48, 638 (1982).

[46]G. Mukhopadhyay, R. K. Kalia, and K. S. Singwi, Phys. Rev. Lett. 34, 950 (1975).

[47]K. Awa, H. Yasuhara, and T. Asahi, Phys. Rev. B 25, 3670 (1982); 25, 3687 (1982).

[48]See the references in Ref. 1.

[49]K. S. Singwi, M. P. Tosi, R. H. Land, and A. Sjölander, Phys. Rev. 176, 589 (1968).

[50]B. Goodman and A. Sjölander, Phys. Rev. B 8, 200 (1973).

[51]W. Macke, Z. Naturforsch. 5a, 192 (1950).

[52]M. Gell-Mann and K. A. Brueckner, Phys. Rev. 106, 364 (1957).

[53]D. F. DuBois, Ann. Phys. (N.Y.) 7, 174 (1959).

[54]W. J. Carr, Jr. and A. A. Maradudin, Phys. Rev. 133, A371 (1964).

[55]D. Y. Kojima and A. Isihara, Z. Phys. B 25, 167 (1976).

[56]N. H. March, Phys. Rev. 110, 604 (1958).

[57]P. N. Argyres, Phys. Rev. 154, 410 (1967).

[58]N. Iwamoto, Institute for Theoretical Physics (Santa Barbara) Report No. NSF-ITP-83-126 (unpublished).